A Preclinical Assessment of ^{89}Zr-atezolizumab Identifies A Requirement For Carrier Added Formulations Not Observed With ^{89}Zr-C4

Anna Moroz[1,2], Lee, Chia-Yin[3], Yung-hua Wang[2], Jeffrey C. Hsiao[2], Natalia Sevillano[4], Charles Truillet[5], Charles S. Craik[4,6], Lawrence Fong[6,7], Cheng-I Wang[3], Michael J. Evans[2,4,6,*]

[1]Skolkovo Institute of Science and Technology, Skolkovo Innovation Center, 3 Nobel St, Moscow, Russia, 143026

[2]Department of Radiology and Biomedical Imaging, University of California San Francisco 505 Parnassus Ave, San Francisco CA 94143

[3]Singapore Immunology Network, Agency for Science, Technology and Research (A*STAR), 8A Biomedical Grove Immunos #03-06, Biopolis Singapore 138648

[4]Department of Pharmaceutical Chemistry, University of California San Francisco 505 Parnassus Ave, San Francisco CA 94143

[5]Imagerie Moleculaire In Vivo, INSERM, CEA, Univ. Paris Sud, CNRS, Universite Paris Saclay, CEA-Service Hospitalier Frederic Joliot, Orsay France, 94100

[6]Helen Diller Family Comprehensive Cancer Center, [7]Department of Medicine, University of California San Francisco, 505 Parnassus Ave, San Francisco CA 94143

[*]To whom the correspondence should be addressed: Michael J. Evans

michael.evans@ucsf.edu

Figure S1. Characterization and radiolabeling of DFO conjugated atezolizumab. **A.** A plot showing the displacement of ^{89}Zr from ^{89}Zr-DFO-atezolizumab as a function of added cold $ZrCl_4$. Using this plot, the average number of chelates per molecule of atezolizumab was determined to be 2.26. **B.** Instant thin layer chromatography (iTLC) traces from the radiosynthesis of ^{89}Zr-atezolizumab. At top is shown the crude reaction after 120 min, and below is purified ^{89}Zr-atezo after size exclusion chromatography. The arrow is centered over the position of expected migration of unconjugated ^{89}Zr-oxalate.

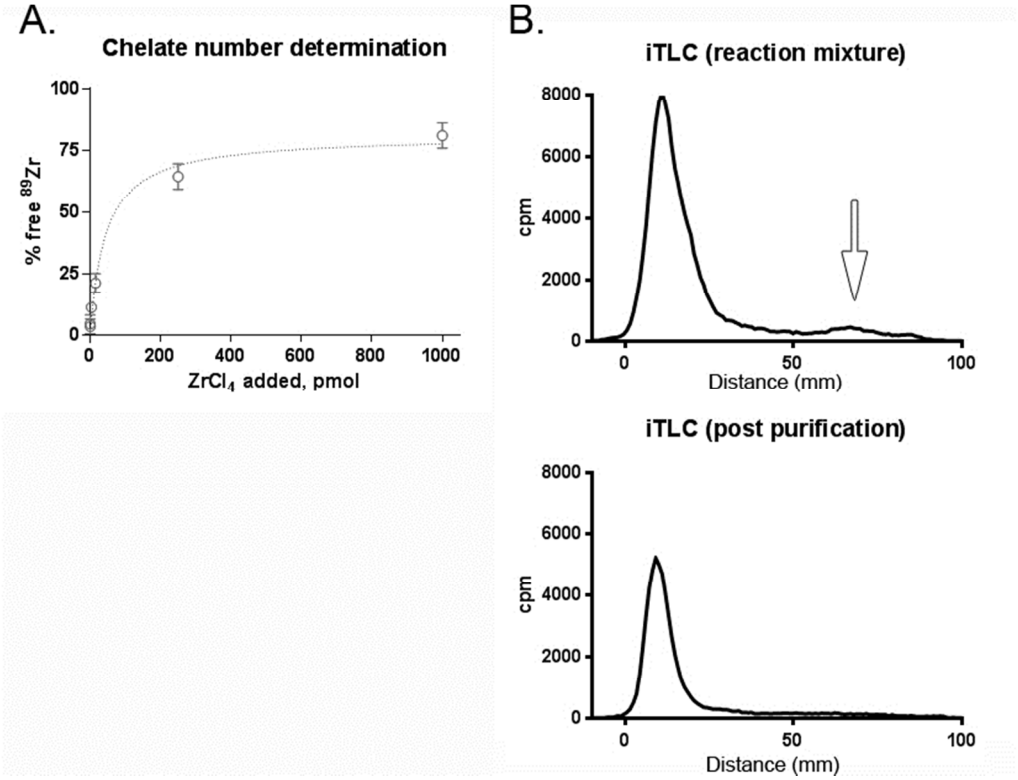

Figure S2. A. A summary of the biodistribution of ^{89}Zr-atezo over time (out to 96 hour post injection) in intact male C57Bl/6J mice bearing subcutaneous B16 F10 tumors. Data from each time point represents mean ± standard deviation for cohort sizes of n = 4. Lg. Int. = large intestine, Sm. Int. = small intestine. B. A summary of the biodistribution of ^{89}Zr-C4 over time in intact male C57Bl/6J mice bearing subcutaneous B16 F10 tumors. The data is rendered from our previously disclosed work[1].

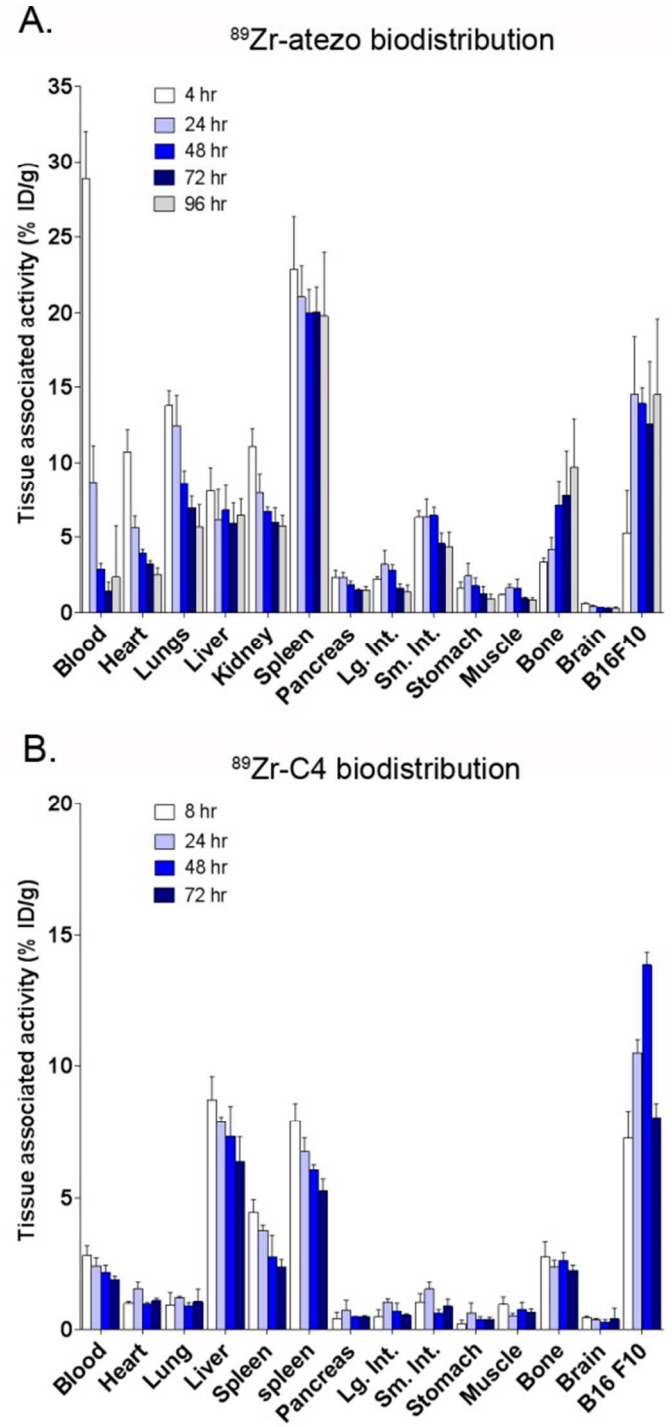

Figure S3. Biodistribution data from select tissue compartments in tumor bearing intact male C57Bl/6J mice 48 hours post injection of ^{89}Zr-atezo or heat denatured (HD) ^{89}Zr-atezo. Heat denaturation substantially decreased tumor-associated ^{89}Zr-atezo. Heat denaturation also reduced levels of ^{89}Zr-atezo in blood, muscle, and bone. Data from each time point represents mean ± standard deviation for cohort sizes of n = 4.

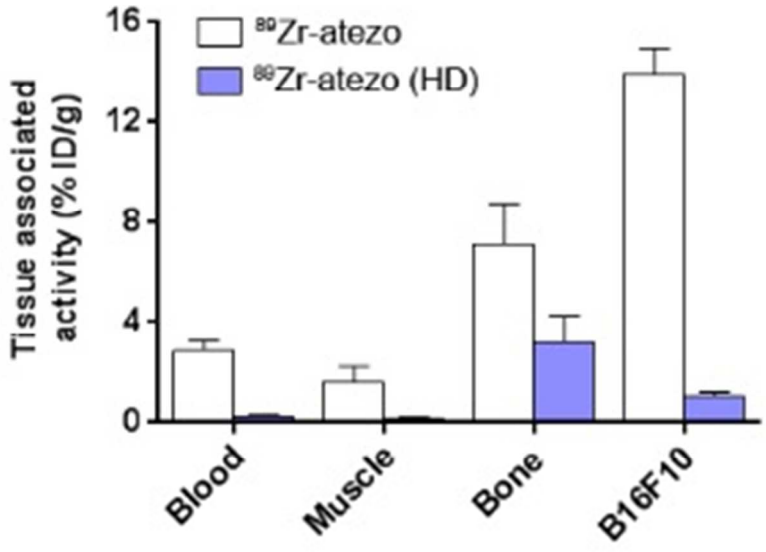

Figure S4. A. A summary of the biodistribution of ^{89}Zr-atezo over time in immunocompromised intact male nu/nu mice bearing subcutaneous H1975 tumors. Data from each time point represents mean ± standard deviation for cohort sizes of n = 4. Lg. Int. = large intestine, Sm. Int. = small intestine. B. A summary of the biodistribution of ^{89}Zr-C4 over time in intact male nu/nu mice bearing subcutaneous H1975 tumors. The data is rendered from our previously disclosed work[1].

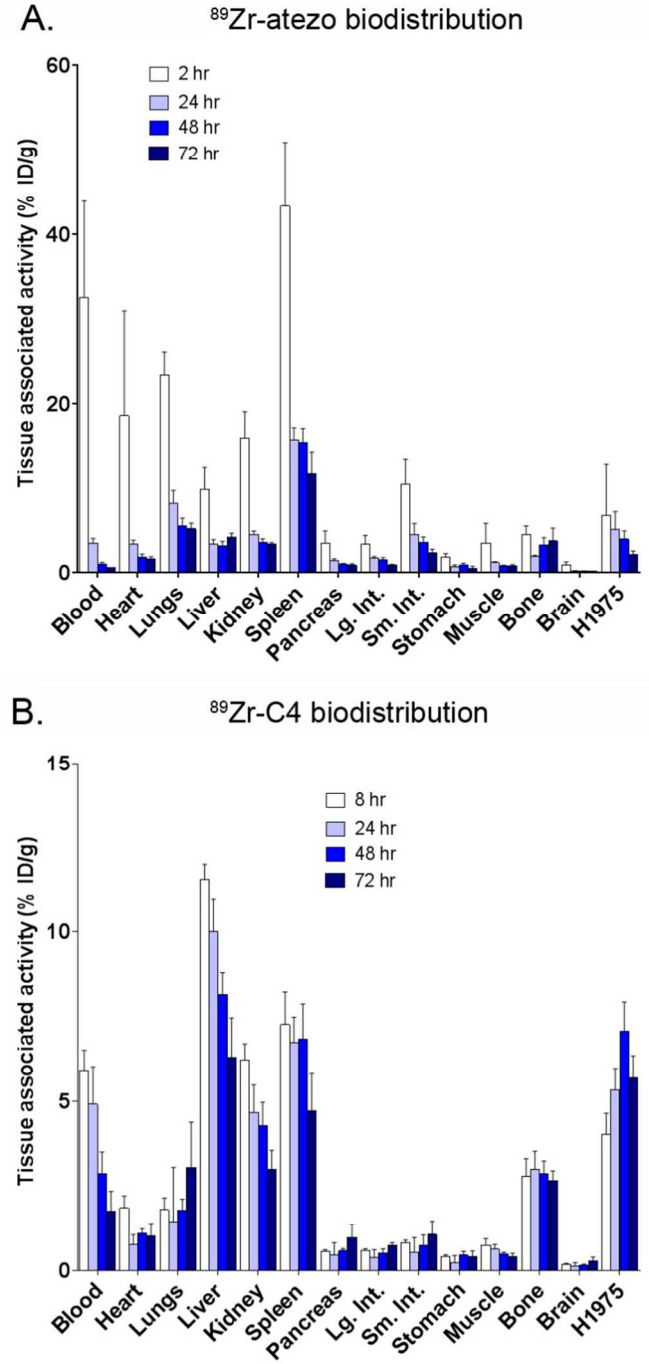

Figure S5. A summary of the biodistribution of ^{89}Zr-atezo at 48 hours post injection in tumor bearing immunocompetent intact male C57Bl/6J mice injected with ^{89}Zr-atezo, ^{89}Zr-atezo + 15X naked atezo, or ^{89}Zr-atezo + 15X IgG1 isotype control. Data from each time point represents mean ± standard deviation for cohort sizes of n = 4. Lg. Int. = large intestine, Sm. Int. = small intestine.

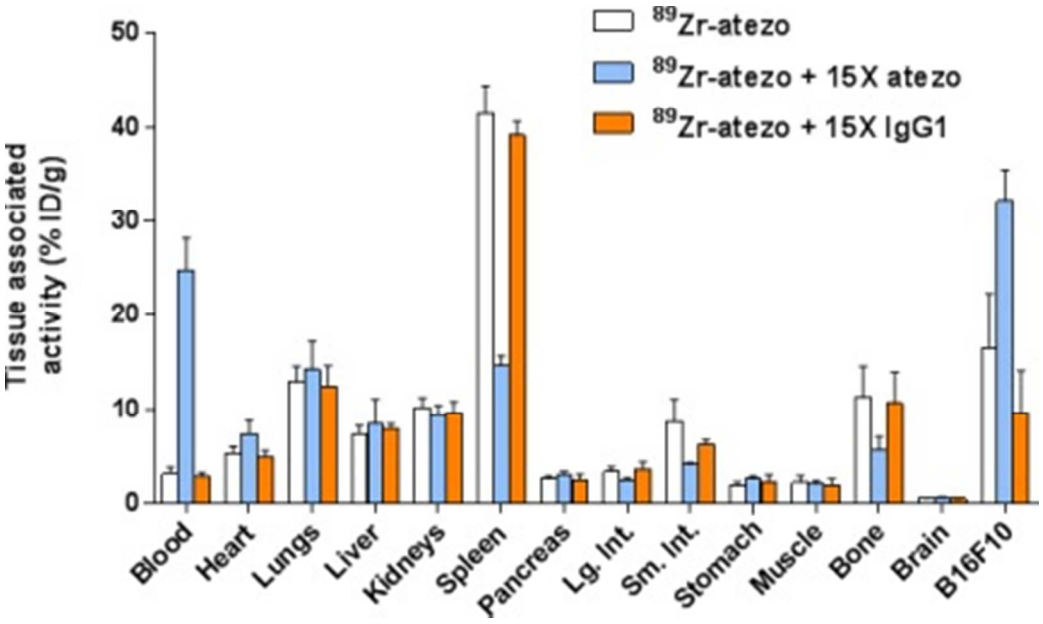

Figure S6. A summary of the biodistribution of ^{89}Zr-atezo at 48 hours post injection in tumor bearing immunocompromised intact male nu/nu mice exposed to carrier free and carrier added formulations of the radiotracer. 15x molar excess of unlabeled atezo was co-injected as carrier. Data from each time point represents mean ± standard deviation for cohort sizes of n = 4. Lg. Int. = large intestine, Sm. Int. = small intestine.

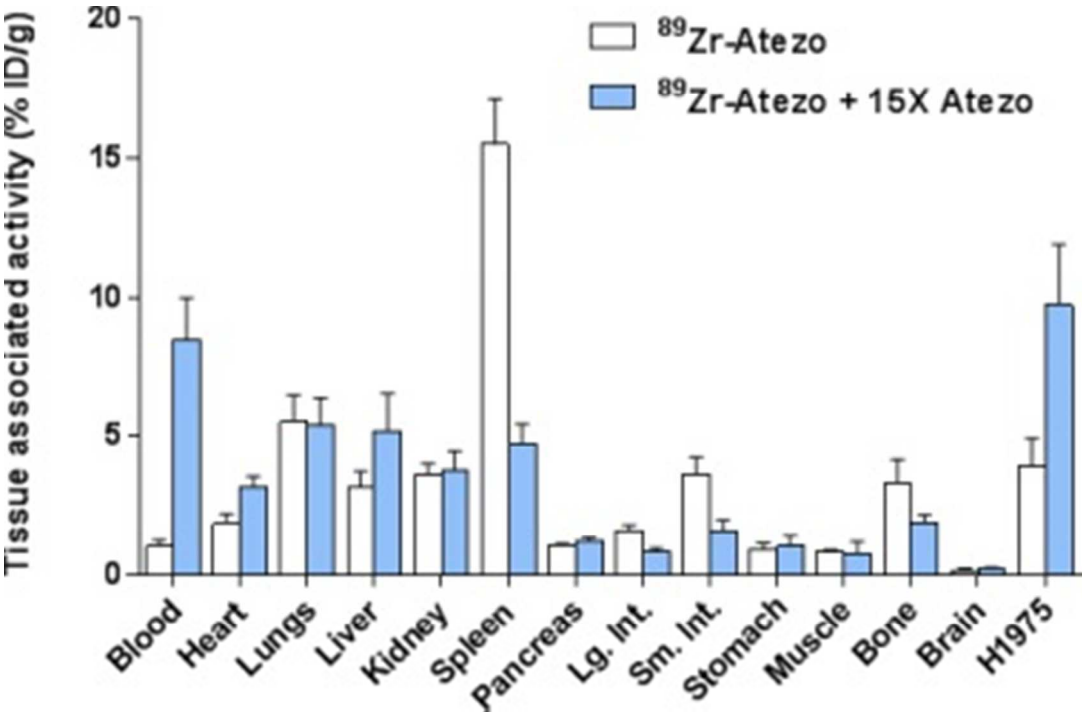

Figure S7. A bar graph representing the percentage of cell bound ^{89}Zr-atezo after incubation alone, or in combination with 10X atezo or C4. The data are expressed as a percentage of bound activity compared to total activity added to the B16 F10 cells, and normalized to cell number. The incubation was performed for 30 min at 4^{o} C. Data represent the mean ± standard deviation from 4 wells per treatment arm. *P<0.01

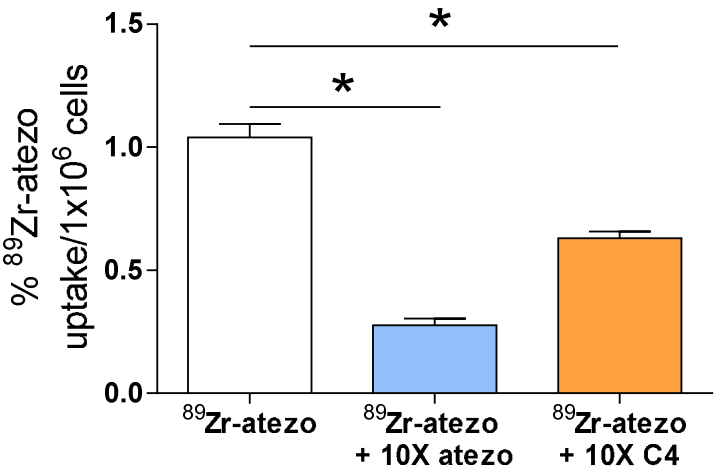

References:

(1) Truillet, C.; Oh, H. L. J.; Yeo, S. P.; Lee, C. Y.; Huynh, L. T.; Wei, J.; Parker, M. F. L.; Blakely, C.; Sevillano, N.; Wang, Y. H.; et al. (2018) Imaging PD-L1 Expression with ImmunoPET. *Bioconjugate chemistry 29*, 96-103.